




Proceeding Paper

Remote Sensing Biological Pump Potential: Plankton Spatio-Temporal Modelling in the Philippine Seas with Emphasis on the Effects of Typhoons [†]

Khim Cathleen Saddi ^{1,2,3,4,*}  and Leni Yap-Dejeto ^{1,5}

¹ Faculty of Management and Development Studies, University of the Philippines Open University, Los Baños 4031, Philippines; lgyapdejeto@up.edu.ph

² Scuola Universitaria Superiore IUSS Pavia, 27100 Pavia, Italy

³ Dipartimento di Ingegneria Civile, Edile e Ambientale (DICEA), Università degli Studi di Napoli Federico II, 80138 Napoli, Italy

⁴ Department of Civil Engineering and Architecture, Ateneo de Naga University, Naga 4400, Philippines

⁵ Division of Natural Sciences and Mathematics, University of the Philippines Tacloban College, Tacloban City 6500, Philippines

* Correspondence: khim.saddi@iusspavia.it

[†] Presented at The 5th International Electronic Conference on Remote Sensing, 7–21 November 2023; Available online: <https://ecrs2023.sciforum.net/>.

Abstract: This study focuses on the quantification and forecasting of the biological pump potential in the Philippine seas, specifically inside the Exclusive Economic Zone (EEZ). Variabilities and disturbances that might potentially influence ocean productivity such as increased sea surface temperature (SST), and the high frequency of typhoons in the Philippines were investigated. CHL and SST spatio-temporal maps were used to provide visualization for the trends and phenomena before, during, and after typhoon occurrence for the years 2019–2021. Integrating the NASA Ocean Color data of CHL and SST with typhoon tracks, the biological pump potential annual estimate was generated.

Keywords: image processing; biological pump potential; environmental monitoring; remote sensing; forecasting planktons; plankton carbon sequestration



Citation: Saddi, K.C.; Yap-Dejeto, L. Remote Sensing Biological Pump Potential: Plankton Spatio-Temporal Modelling in the Philippine Seas with Emphasis on the Effects of Typhoons. *Environ. Sci. Proc.* **2024**, *29*, 79. <https://doi.org/10.3390/ECRS2023-16862>

Academic Editor: Riccardo Buccolieri

Published: 8 February 2024



Copyright: © 2024 by the authors. Licensee MDPI, Basel, Switzerland. This article is an open access article distributed under the terms and conditions of the Creative Commons Attribution (CC BY) license (<https://creativecommons.org/licenses/by/4.0/>).

1. Introduction

In regulating the atmospheric CO₂ concentration, the ocean plays a vital role in the Earth's carbon cycle [1]. There are six (6) ocean biological carbon pumps (OBCPs) that comprise the downward pumping of biogenic carbon to the deep ocean [2], estimated to be at between 5 and 14 Pg C y⁻¹ [3,4]. These include the mixed layer pump, the Eddy subduction pump, the large-scale subduction pump, Ekman pumping, and animal-mediated pumps, and the vertical migration of zooplankton [5]. Some animals like fish and jellyfish, which are larger than zooplankton, may also contribute to these animal-mediated pumps [6]. Presently, various techniques have been conducted to monitor and understand the dynamics of these processes in space and time, which is also critical in global climate processes [7].

Geographically situated in the typhoon belt of the Pacific, the Philippines experiences an average of 20 typhoons per year [8]. The archipelago, which consists of over 7000 islands and islets, is clustered into three main island groups, Luzon, Visayas and Mindanao. The Southern parts of Luzon and Visayas islands are the most hard-hit in terms of typhoons, among other natural disasters experienced in the country. Given these threats, the Philippines has a high biodiversity including numerous flora and fauna endemic to the archipelago, hence the need to advance our understanding of the marine environment to improve monitoring and intervention efforts in the future.

The use of remote sensing, similar to various environmental monitoring, provides an avenue to expand the understanding of the OBCPs, from traditional ship-based Net Primary Production (NPP) [9,10] point measurements, to space and time covering the entire ocean [1]. This paper presents a viable and low-cost option to estimate the available NPP-exploiting remote sensing data products.

2. Materials and Methods

False color representations of satellite data were extracted from the NASA Ocean Color website. Specifically, the maps used included 8-day data of both CHL and SST from the Level 1 and 2 browser, with a total of 276 images for 2019–2021. These data were produced under NASA’s Earth Observing System Data and Information System (EOSDIS). NASA’s CHL uses an algorithm derived from the in situ measurements of CHL-a and remote sensing reflectances (Rrs) captured by satellite sensors using the band range 440–670 nm [11]. The SST was derived from long-wave infrared (LWIR) bands in MODIS and VIIRS sensors with an algorithm based on a modified nonlinear SST algorithm developed by [12] and recently by [13].

The region of interest (ROI) considered is specific to the extent of the Philippine Exclusive Economic Zone (EEZ) for data cleaning and processing. Instead of total pixel removal, cloud covers represented by black pixels were all replaced by non-black neighboring pixels.

To simplify the analysis of the CHL trends and plankton productivity, the EEZ of the archipelago was subdivided into 4 quadrants (also represented by the transect lines in covering the main seas around the country: the Philippine Sea (T1&T2), West Philippine Sea (T4), and Sulu Sea (T3) (see Figure 1). Coordinates of the four (4) transect lines were used to extract the RGB data of all 75 × 75 px images (CHL and SST).

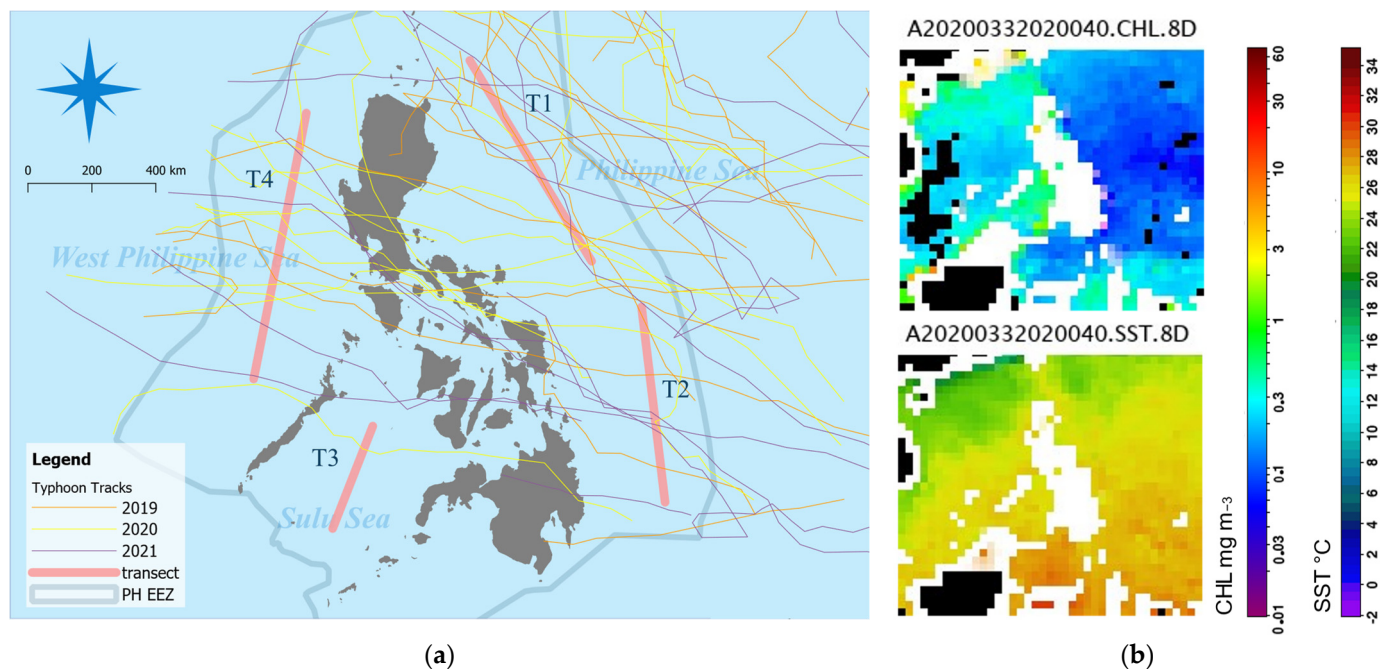


Figure 1. Visualization of the (a) Philippine Tropical Cyclone tracks for the years 2019–2021, and sample NASA false color maps for (b) CHL/SST. CHL peak month map (February 2020).

Image processing and machine learning using Python and Matlab were utilized to generate the 75 × 75 spatio-temporal 8-day maps for the years 2019–2021. K-nearest neighbor (KNN) was used to facilitate classification of the map data and extraction of both the CHL and SST values based on NASA Color scales.

Spatio-temporal CHL abundance was compared with SST variability and typhoon occurrence (pre, during and after) to look for trends in both short- and long-term periods. CHL and SST linear relationships were also checked for possible correlations.

Using the spatio-temporal model, mainly considering SST and integrating possible typhoon occurrence as buffer, the forecast for the Philippine biological pump potential was generated.

3. Results

High productivity occurs mainly in the West Philippine Sea (Quadrant 4), and Sulu Sea (Quadrant 3), as shown in Figure 1b.

3.1. Spatio-Temporal Relationships of CHL, Typhoons and SST

The typhoon season in the Philippines usually begins in June but typhoons may occur as early as January, as was the case in 2019. However, the Philippine Atmospheric, Geophysical, and Astronomical Services Administration (PAGASA) started detecting typhoons entering in the Philippine Area of responsibility only in the month of May for the year 2020, with high-intensity typhoons occurring in the last quarter of the year and primarily in Luzon and Visayas. The opposite can be said for 2021 with typhoons both for the 3rd and 4th quarter but mostly in the Visayas and Mindanao area. High-intensity typhoons occur in Luzon (2019), Luzon and Visayas (2020) and Visayas and Mindanao (2021) with winds as high as over 250 kph, 315 kph, and 280 kph, respectively. In fact, back in 2020, there was even a series of typhoons that hit the Bicol Region in a span of only 3 weeks, led by the infamous Super Typhoon Rolly.

It was highly evident that when typhoons Goring and Betty (2019), Marce and Carina (2020), and Kiko, Jolina, Maring, and Nando (2021) traversed near transect 1, the CHL value dropped, as shown in Figure 2. In transect 2, this was also true with Ambo (2020), but with Liwayway (2019), Bising (2021) and Odette (2021), there was no change in the CHL value, even though they were both high-intensity typhoons. On the other hand, it was surprising to observe that when typhoons Amang (2019) and Auring (2021) traversed near transect 2, the CHL value increased [10].

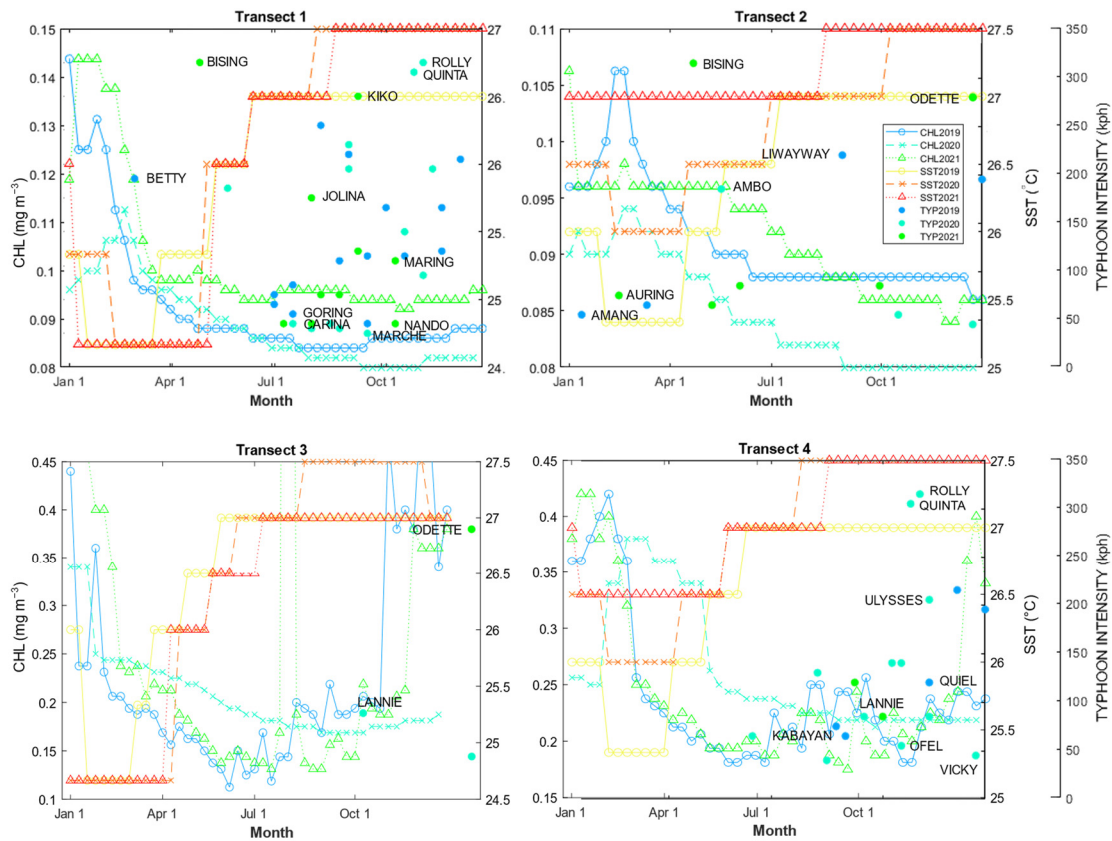


Figure 2. Time series plot of CHL, SST and typhoons for all transect lines for 2019–2021.

While there was minimal typhoon crossing in transect 3, except for Odette (2021) with increased CHL, transect 4 is rather peculiar since the CHL value increased after the occurrence of Kabayan (2019), Quiel (2019), Ofel (2020), but decreased after Lannie (2021).

Each transect showed a different trend. In transect 1, a steep decrease in CHL was observed with decreasing SST for January–March (2019–2021), while a steady decrease in CHL with increasing SST was observed from April onwards for 2019–2020 and almost no change in CHL was reported for 2021. Interestingly, in transect 2, decreasing SST correlated with increasing and decreasing CHL for February–March (2019–2020), while decreasing CHL correlated with increasing SST from April onwards, which is also evident for the 2nd half of the year 2021. Transect 3 did not show a clear trend between CHL and SST.

There are three different trends that can be observed in transect 4. In 2019, CHL markedly decreased with decreasing SST from February to March, while the opposite was observed in 2020, with CHL increasing with decreasing SST. On the other hand, in 2021, increasing and decreasing CHL correlated with decreasing SST for January–April. However, for the second threshold of the year, increasing SST and decreasing CHL went hand-in-hand from April/May onwards (2019–2020).

The CHL and SST regression results showed a weak linear relationship between CHL and SST using all the data from 2019 to 2021, and individual yearly data (true for 2019 and 2021). Yet, it was surprising that a single high R2 value ($R_{2020} = 0.81$) was observed with the occurrence of typhoons, specifically Super Typhoon Rolly (see Table 1).

Table 1. Regression results for different data input periods (2019–2021).

Year	R2	Adj R2	STD Error	Data Range Error
2019	0.497350775	0.485926929	0.010314718	0.172631256
2020	0.813471554	0.809133683	0.003874051	0.11920158
2021	0.420219238	0.407042402	0.011789143	0.227809524
2019–2021 *	0.423529973	0.419227958	0.010920877	0.171307876

* Results reflect total ungrouped data.

3.2. Ocean Net Primary Productivity (NPP) Estimation

The Vertically Generalized Production Model (VGPM), a widely used NPP model, was utilized to generate the NPP in all four quadrants of the Philippine EEZ following the transect assignment. VGPM was first described by [14], and since then, this model has been utilized and further improved with the development of carbon-based NPP [15].

The NPP model used is represented by the following equation:

$$npp = chl \times pb_opt \times day\ length \times f(irr) \times z_eu, \tag{1}$$

which follows the convention of the original VGM model. Both the CHL and SST data were previously generated. The $f(irr)$ is the photosynthetically active radiation (PAR) function that was downloaded from the NASA Ocean Color website [16], while pb_opt is a polynomial of 7th order, which varies depending on the sea surface temperature.

There is a general trend of high levels of NPP during December–January (Q1–Q3), which are rainy and cold months in the Philippines. However, a peak anomaly was recorded for July of 2021 ($NPP_{Peak2021} = 2235.5\ mgC\ m^{-2}\ day^{-1}$). There is a single downward curve in July–August (Q1–Q3), while a double downward curve can be observed May–June and November–December (Q4) (see Figure 3). Without removing the anomaly, the NPP annual value for 2021 was estimated at approximately $0.34\ PgC\ y^{-1}$.

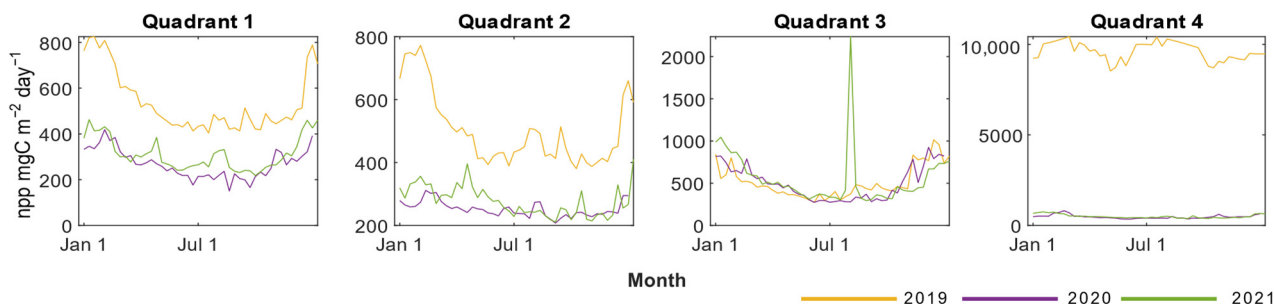


Figure 3. Net primary production estimate for 2019–2021.

4. Discussion and Conclusions

This study presented a low-cost methodology to provide an overview of the “where” and “when” of ocean productivity in response to typhoon occurrences in the Philippines, which is one of the hardest hit countries in the world in terms of cyclones.

It is encouraging that typhoon frequency is not heavily affecting productivity, as much as SST. In fact, there are instances where productivity increases after typhoon occurrence. A similar observation in China was recorded, which may be attributed to the nutrient mixing and upwelling after typhoon passage [17].

Interestingly, a strong linear relationship between CHL and SST was observed for the year 2020. Since it was the year of the pandemic, it is possible that less anthropogenic activities might have minimized the CHL variability. The varying value of R2 considering different data groups of CHL and SST suggested that other factors may influence CHL variability, such as anthropogenic activities. Moreover, the importance of close monitoring in quadrant 3 (Sulu Sea), and quadrant 4 (West Philippine Sea) should be prioritized given the relatively high productivity in these regions.

Limited to the spatial resolution of Landsat 8 (30 m swath width), the results may represent an underestimate of the actual phytoplankton productivity. Hence, it is highly recommended to explore the use of Sentinel-2 data to improve the spatial resolution in analyses. Although typhoon occurrence poses no major threat to planktonic productivity, recent literature suggests that fast transport of organic compounds via typhoon-induced urban runoff could potentially make the ocean, which has long been considered a sink, now also a carbon source [18]. This coupling effect of typhoons is not yet extensively understood [19] and more research is required in this direction. The NPP annual estimate suggests that the PH EEZ is causing a carbon sink; however, the NPP VGM product from the ocean productivity website says otherwise ($NPP_{OP2021} = -0.64 \text{ PgC y}^{-1}$ based on monthly scale), despite using the same model. It would be beneficial to obtain NPP validation with ground truths, which was not presented in this paper.

These uncertainties should be explored in future work including bioindicators for stress in oceans, and potentially activities in the river corridor, to better understand the microprocesses that influence planktonic activity both at the macro and microscale.

Supplementary Materials: The following supporting information can be downloaded at: Philippine typhoon tracks are available on the DOST PAGASA website [8].

Author Contributions: Conceptualization and methodology, K.C.S. and L.Y.-D.; software, validation, formal analysis, investigation, resources, data curation, and writing—original draft preparation, K.C.S.; writing—review and editing, K.C.S. and L.Y.-D.; visualization, K.C.S.; supervision, L.Y.-D.; project administration, K.C.S. All authors have read and agreed to the published version of the manuscript.

Funding: This research received no external funding.

Institutional Review Board Statement: Not applicable.

Informed Consent Statement: Not applicable.

Data Availability Statement: The CHL and SST can be downloaded from the NASA Ocean Color website, and the NPP-related parameters from the Ocean Productivity website.

Acknowledgments: The main author wishes to acknowledge Mari as a significant source of inspiration.

Conflicts of Interest: The authors declare no conflicts of interest.

References

1. Brewin, R.J.W.; Sathyendranath, S.; Platt, T.; Bouman, H.; Ciavatta, S.; Dall’Olmo, G.; Dingle, J.; Groom, S.; Jönsson, B.; Kostadinov, T.S.; et al. Sensing the ocean biological carbon pump from space: A review of capabilities, concepts, research gaps and future developments. *Earth-Sci. Rev.* **2021**, *217*, 103604. [CrossRef]
2. Claustre, H.; Legendre, L.; Boyd, P.W.; Levy, M. The Oceans’ Biological Carbon Pumps: Framework for a Research Observational Community Approach. *Front. Mar. Sci.* **2021**, *8*, 780052. [CrossRef]
3. Laws, E.A.; Falkowski, P.G.; Smith, W.O., Jr.; Ducklow, H.; McCarth, J.J. Temperature effects on export production in the open ocean. *Glob. Biogeochem. Cycles* **2000**, *14*, 1231–1246. [CrossRef]
4. Najjar, R.G.; Keeling, R.F. Mean annual cycle of the air-Sea oxygen flux: A global view. *Glob. Biogeochem. Cycles* **2000**, *14*, 573–584. [CrossRef]
5. Boyd, P.W.; Claustre, H.; Levy, M.; Siegel, D.A.; Weber, T. Multi-faceted particle pumps drive carbon sequestration in the ocean. *Nature* **2019**, *568*, 327–335. [CrossRef] [PubMed]
6. Pinti, J.; DeVries, T.; Norin, T.; Serra-Pompei, C.; Proud, R.; Siegel, D.A.; Kiørboe, T.; Petrik, C.M.; Andersen, K.H.; Brierley, A.S.; et al. Metazoans, migrations, and the ocean’s biological carbon pump. *Biogeosciences* **2021**, *20*, 997–1009. [CrossRef]
7. Bianchi, A.A.; Bianucci, L.; Piola, A.R.; Pino, D.R.; Schloss, I.; Poisson, A.; Balestrini, C.F. Vertical stratification and air-sea CO₂ fluxes in the Patagonian shelf. *J. Geophys. Res.* **2005**, *110*, C07003. [CrossRef]
8. PAGASA-DOST. Available online: <https://www.pagasa.dost.gov.ph/> (accessed on 1 September 2023).
9. Milutinović, S.; Bertino, L. Assessment and propagation of uncertainties in input terms through an ocean-color-based model of primary productivity. *Remote Sens. Environ.* **2011**, *115*, 1906–1917. [CrossRef]
10. Carr, M.E.; Friedrichs, M.A.M.; Schmeltz, M.; Noguchi Aita, M.; Antoine, D.; Arrigo, K.R.; Asanuma, I.; Aumont, O.; Barber, R.; Behrenfeld, M.; et al. A comparison of global estimates of marine primary production from ocean color. *Deep-Sea Res. Part II Top. Stud. Oceanogr.* **2006**, *53*, 741–770. [CrossRef]
11. Ocean Color. Available online: <https://oceancolor.gsfc.nasa.gov/> (accessed on 1 September 2023).
12. Walton, C.C.; Pichel, W.G.; Sapper, J.F.; May, D.A. The development and operational application of nonlinear algorithms for the measurement of sea surface temperatures with the NOAA polar-orbiting environmental satellites. *J. Geophys. Res.* **1998**, *103*, 27999–28012. [CrossRef]
13. Kilpatrick, K.A.; Podestá, G.; Walsh, S.; Williams, E.; Halliwell, V.; Szczodrak, M.; Brown, O.B.; Minnett, P.J.; Evans, R. A decade of sea surface temperature from MODIS. *Remote Sens. Environ.* **2015**, *165*, 27–41. [CrossRef]
14. Behrenfeld, M.J.; Falkowski, P.G. A Consumer’s Guide to Phytoplankton Primary Productivity Models. *Limnol. Oceanogr.* **1997**, *42*, 1479–1491. [CrossRef]
15. Westberry, T.; Behrenfeld, M.J.; Siegel, D.A.; Boss, E. Carbon-based primary productivity modeling with vertically resolved photoacclimation. *Glob. Biogeochem. Cycles* **2008**, *22*, GB2024. [CrossRef]
16. Ocean Productivity. Available online: <https://sites.science.oregonstate.edu/ocean.productivity/index.php> (accessed on 1 September 2023).
17. Zeng, G.M.; Tang, D. Offshore and nearshore chlorophyll increases induced by typhoon winds and subsequent terrestrial rainwater runoff. *Mar. Ecol. Prog. Ser.* **2007**, *333*, 61–74. [CrossRef]
18. Lao, Q.; Chen, F.; Jin, G.; Lu, X.; Chen, C.; Zhou, X.; Zhu, Q. Characteristics and Mechanisms of Typhoon-Induced Decomposition of Organic Matter and Its Implication for Climate Change. *J. Geophys. Res. Biogeosci.* **2023**, *128*, e2023JG007518. [CrossRef]
19. Chen, F.; Lao, Q.; Lu, X.; Wang, C.; Chen, C.; Liu, S.; Zhou, X. A review of the marine biogeochemical response to typhoons. *Mar. Pollut. Bull.* **2023**, *194 Pt B*, 115408. [CrossRef]

Disclaimer/Publisher’s Note: The statements, opinions and data contained in all publications are solely those of the individual author(s) and contributor(s) and not of MDPI and/or the editor(s). MDPI and/or the editor(s) disclaim responsibility for any injury to people or property resulting from any ideas, methods, instructions or products referred to in the content.